JOURNAL OF MATERIALS SCIENCE 29 (1994) 26–32

Deformation mechanism in α-Cu–Al single crystals with a spherical indentor

Part II *Scratch with steel ball*

S. KOBAYASHI
Department of Mechanical Engineering, Doshisha University, Kamigyoku, Kyoto, Japan
T. HARADA
Food Laboratory, Kanebo Co. Ltd, Kajiwara, Takatsuki, Japan
S. MIURA
Department of Engineering Science, Kyoto University, Sakyoku, Kyoto, Japan

The subject of sliding friction is of great technological importance and has been studied extensively on an engineering basis, but many of the underlying microscopic factors that control friction or wear remain obscure. The present study is part of an effort to relate sliding deformation to the crystal structure of the contacting surfaces. The method was to scratch a steel ball in various crystal directions on an accurately finished surface of Cu–Al single crystals. For a scratch on the (1 1 1) face, the scratched track width and the width of the slipped area were found to be wider in the $[\bar{2}\,1\,1]$ direction than in the $[2\,\bar{1}\,\bar{1}]$. The mechanism of the active slip produced by the scratch can be explained in terms of stress patterns and interactions among the dislocations produced in the subsurface region. The distributions of dislocation density on the cross-section perpendicular to the (1 1 1) face were elucidated.

1. Introduction

An average diameter of metal wear debris produced during the usual wear process is in the range 0.01–0.1 mm. However, Rabinowicz [1] and Soda and Sato [2] have reported that debris with a diameter of the order of 10^{-3} mm has been observed. This indicates that the wear process accompanies the occurrence of wear debris having a diameter of the order of the grain size. So, an elucidation of the microscopic deformation mechanism of the surface layer subjected to repeated contacting stress becomes a matter of serious concern.

From this point of view, studies on the microscopic plastic deformation caused by friction or wear have so far been carried out using single crystals. For example, Bailey and Gwathmey [3] have reported that the damage done by a spherical ball in the surface layer of copper single crystals differs with the scratching direction. Steijn [4] has examined the anisotropy of the frictional damage in relation to frictional force using various kinds of material. Barquins *et al.* [5] have analysed the surface deformation in the case where a sapphire ball is slid over the (1 1 1) face of copper single crystals. However, little work has been done from the viewpoint of the microscopic dislocation level [6–8]. Also, most of the past studies in regard to the deformation in single crystals have been done on the {1 1 0} or {1 0 0} faces of face-centred cubic crystals [3, 9, 10]. However, some problems still remain, in that the slip system of this crystal is {1 1 1}⟨1 1 0⟩, and it is hard to detect the etch pits that correspond to dislocation on the slip planes. When the deformation is produced on one of the slip planes and dislocations are observed, the above-mentioned problems have to be solved if the deformation mechanism is to be grasped precisely and in detail.

In the present study, scratch tests with a steel ball were carried out on the material described in a previous report [9]. The study was performed to examine the width of the scratched track, the appearance of slip traces around the track and the distributions of dislocation density, and to discuss the mechanism of microscopic deformation produced by scratching. The (1 1 1) face was chosen as the scratched surface, and ⟨2 1 1⟩ was chosen as the scratching direction.

2. Experimental procedure

The material used for experiments and the preparation method of the test piece were described in the previous paper [9]. A skeleton diagram of the testing apparatus used for scratching is shown in Fig. 1. In this apparatus the loading device (1) makes a reciprocating motion when the motor (2) is in operation. The set-up of (1) is the same as the one shown in the previous report [9]. Steel balls (3) were set beneath the holder of the test piece (4), and lubricating oil was supplied to reduce as much as possible the friction between the holder (5) and the apparatus itself. Frictional force during the test was measured using the

0022–2461

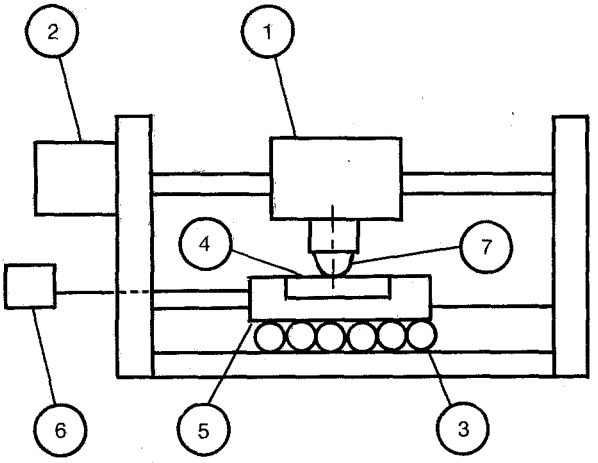

Figure 1 Skeleton diagram of testing apparatus: (1) loading device, (2) motor, (3) steel ball, (4) specimen, (5) holder, (6) detector, (7) indentor.

detector (6) which was directly connected to (5). The same steel ball indentor as that used in the static indentation test [9] was used for the scratch tests. After the ball (7) was statically indented on to the (1 1 1) face of the test piece, the scratch was made at a constant feeding speed of 0.5 mm s^{-1}.

The scratch tests were carried out under a load in the range 0.3–10.0 N. All the tests were performed at a temperature of 20° C and an air humidity of about 40%. The slip traces formed on either side of the scratched track were examined, and then each surface was etched every time a thin layer of 10 μm thickness was removed by electrolytic polishing, so as to examine the dislocation patterns beneath the track. Furthermore, it was investigated how the plastic deformation patterns formed by scratching relate to those formed by static indentation [9]. Interactions between two dislocation motions which are active on the different cubic faces and meet each other at the intersections were also studied.

3. Experimental results and discussion

3.1. Deformations and slip systems on the (1 1 1) face

Figs 2a and 3a show the appearances of the (1 1 1) surfaces scratched under a load of 0.3 N in the $[\bar{2}\,1\,1]$ and $[2\,\bar{1}\,\bar{1}]$ directions, respectively. The width of the scratched track in these figures is estimated to be 65 and 75 μm, respectively. Such anisotropy in the deformation caused by different directional scratches was also observed under other loads.

In these figures the slip traces in the $\langle 0\,1\,1\rangle$ direction which prove the activity of dislocations on the (1 1 1) face can be slightly observed. The etch pit distribution and slip systems around the track can be detected by surface etching. Figs 2b and 3b show the etched appearances of the surfaces shown in Fig. 2a and 3a, respectively.

Since the distribution density of the etch pits beneath the track is at a considerably higher level, the slip system of the traces cannot be confirmed. In f.c.c. crystals the $(1\,\bar{1}\,1)$ and $(1\,1\,\bar{1})$ faces which are the principal slip planes are located in a coordinate relation to both $[\bar{2}\,1\,1]$ and $[2\,\bar{1}\,\bar{1}]$ directions. Therefore, slip traces show symmetrical patterns with respect to the scratched track as shown in Fig. 3. Fig. 4 shows the relations between scratched width and load, and Fig. 5 represents the relations between load and width of slipped area in which etch pits are detected. As shown in these figures, while the width of slipped area increases in proportion to the load, the width of scratched track becomes smaller in its rate of increase as the load increases.

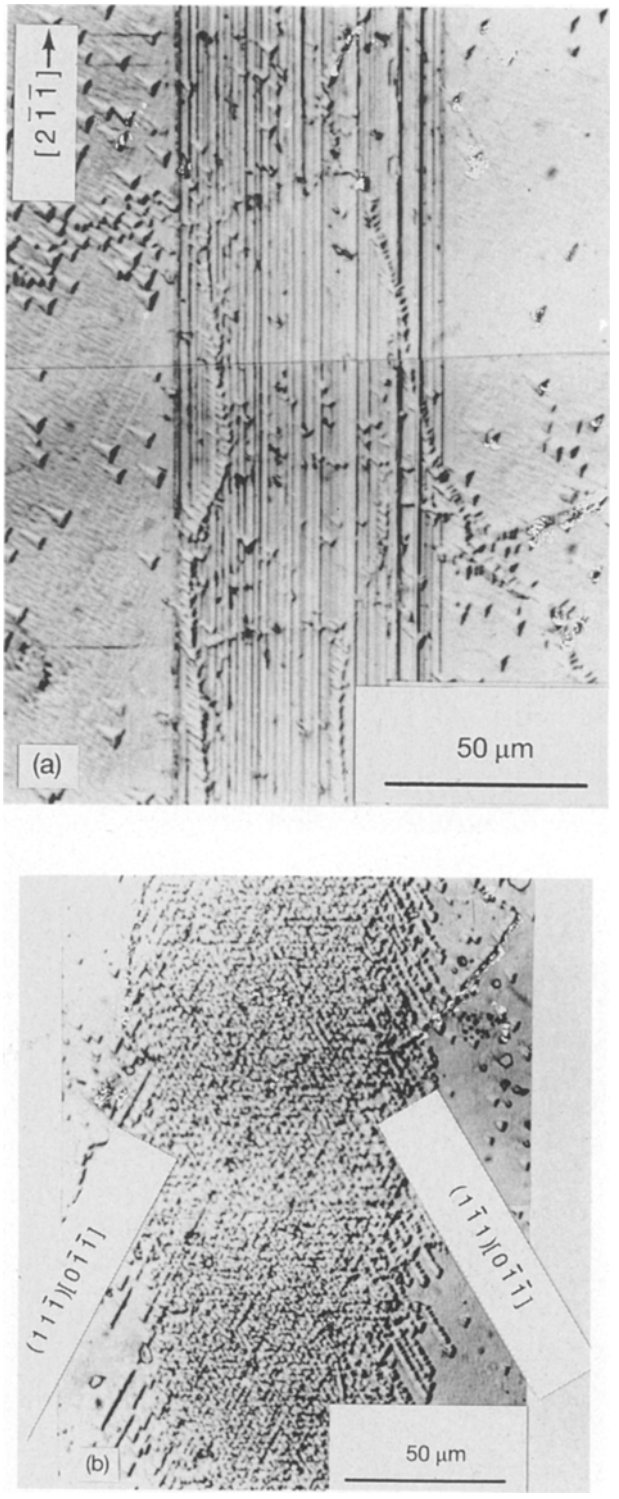

Figure 2 Appearance of scratched surface with track and slip traces under load of 0.3 N. Slip systems of traces are shown with Miller indices. Scratched direction: (a) $[\bar{2}\,1\,1]$, (b) $[2\,\bar{1}\,\bar{1}]$.

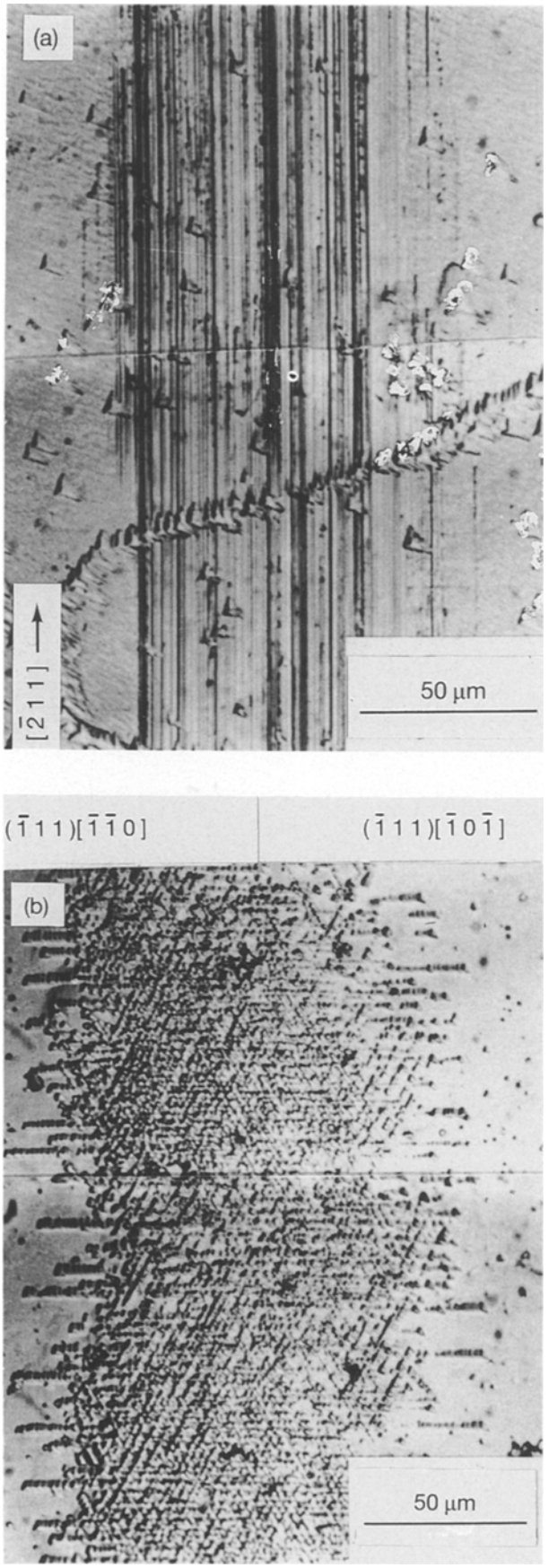

Figure 3 Appearance of etched surface. scratched direction: (a) [2̄ 1 1], (b) [2 1̄ 1̄].

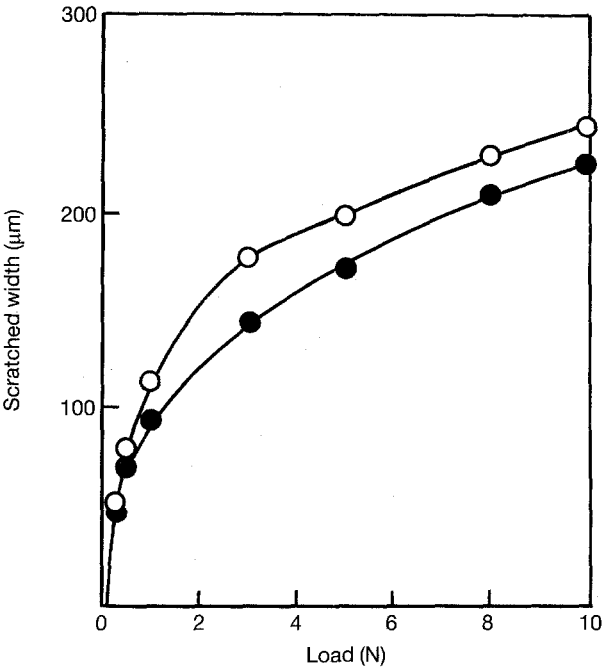

Figure 4 Relation between width of scratched track and applied load. Scratched direction: (○) [2̄ 1 1], (●) [2 1̄ 1̄].

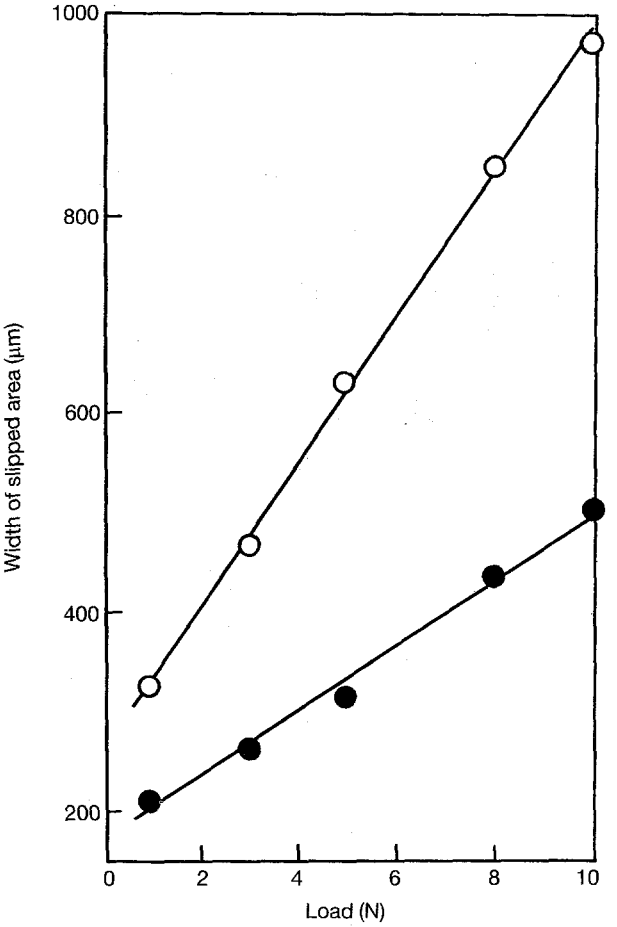

Figure 5 Relation between width of slipped area and applied load. Scratched direction: (○) [2̄ 1 1], (●) [2 1̄ 1̄].

In other words, the magnitude of macroscopic deformation on the scratched surface does not always correspond proportionately to that of microscopic deformation at the dislocation level. The same results were clearly obtained in the case of a [0 1̄ 1] scratch as shown in Fig. 6.

The slip planes and slip directions differ with the directions of the acting stress vectors; therefore aspects

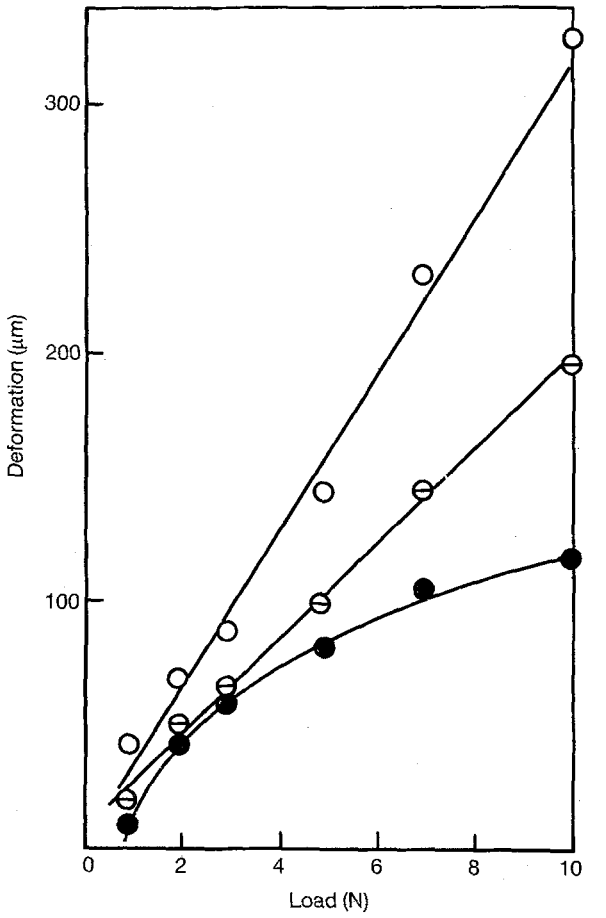

Figure 6 Relation between applied load and plastic deformation produced by scratches. (○) Width of slipped area, (⊖) depth of slipped area, (●) width of scratched track.

of deformations also differ with the scratched direction. This can be seen in Figs 7 and 8. These figures show a scratched track and slip traces around it formed by $[\bar{2}\,1\,1]$ and $[2\,\bar{1}\,\bar{1}]$ scratches, respectively. Slip planes and these directions are shown with Miller indices. In comparison with the case of a load of 0.3 N, the slip traces in every direction cover a wide area, and are formed more clearly. Both the width of the scratched track and that of the slipped area in the $[\bar{2}\,1\,1]$ scratch are certainly larger than those in the $[2\,\bar{1}\,\bar{1}]$ scratch. Especially with respect to the latter case, this tendency becomes more conspicuous as the load increases.

The symbol A in Fig. 7 shows an indent formed by an indentor before the start of the scratch. The slip traces around it are formed in the same triangular patterns as in the indenting case [9]. Slip traces marked with the letters c, d in Fig. 7 and b, c in Fig. 8 are observed. These are produced by dislocations operating on the slip planes $(1\,\bar{1}\,1)$ and $(1\,1\,\bar{1})$, respectively. The directions of slip on these planes differ from the scratched directions, as shown in these figures. These are the principal slip systems in these two directional scratches. In addition, the slip traces b in Fig. 7 and a in Fig. 8, which prove that dislocations were active on another principal plane $(\bar{1}\,1\,1)$, are observed on either side and in front of the track.

When a steel ball is scratched on a crystal surface, the material is subjected to another force which contributes to the pile-up around the front area of the

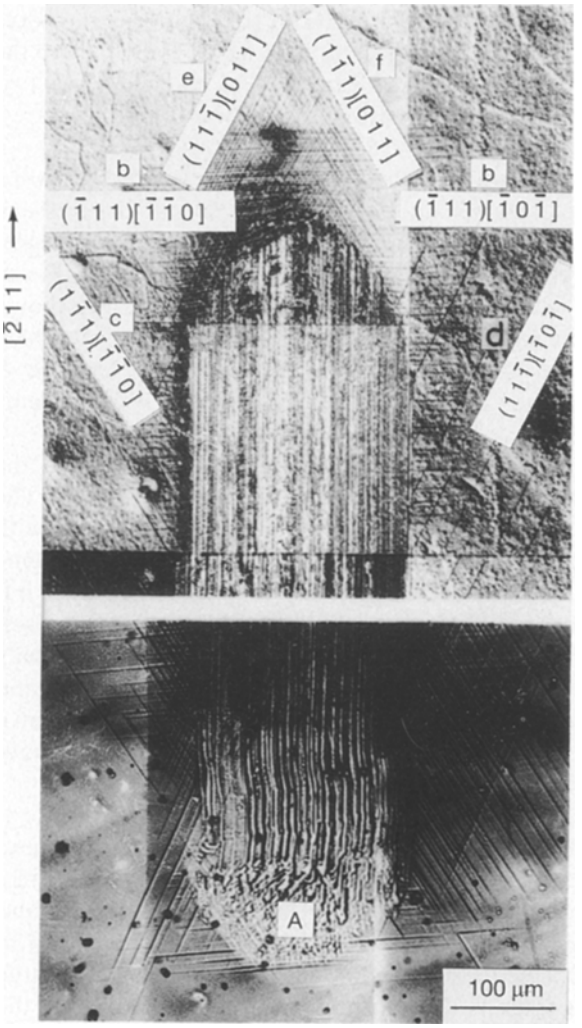

Figure 7 Scratched track with slip traces under load of 8.0 N on $(1\,1\,1)$ face in $[\bar{2}\,1\,1]$ direction.

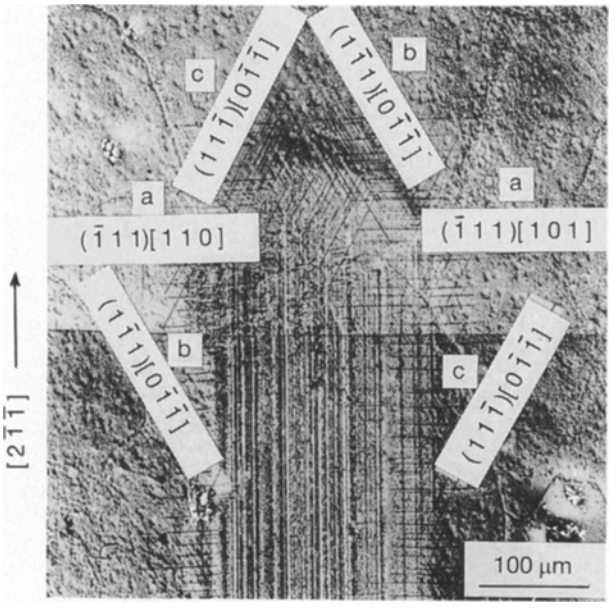

Figure 8 Scratched track with slip traces under load of 8.0 N on $(1\,1\,1)$ face in $[2\,\bar{1}\,\bar{1}]$ direction.

indentor in addition to the combination of frictional force and normal force. It can be called "shearing force of dig-out". The shear stresses which contribute to the slip of crystal faces can thus be classified into two types that act upward and downward. Let these stresses be replaced by ***P*** and ***Q***.

Fig. 9a and b show the slip systems and shear stress vectors which are expected in the crystal in the case of scratching in the $[\bar{2}\,1\,1]$ and $[2\,\bar{1}\,\bar{1}]$ directions, respectively. Since the indentor is spherical in shape, ***P*** and ***Q*** act in the directions indicated by the arrows shown on each slip plane. Slip planes of the crystal which correspond to slip traces marked with the letters b, c, d, e and f in Fig. 7 are shown in Fig. 9a with the same respective letters.

Slip traces b, c and d are produced due to the influence of stress ***P***, and e, f are due to stress ***Q***. The slip traces a, b and c shown in Fig. 8 are produced with dislocation activities on planes which have the same Miller indices as in the case of the $[\bar{2}\,1\,1]$ scratch, but the slip directions are different. By collating this result with the model of Fig. 9b, it is confirmed that only trace a is produced by the stress ***Q***, and that b and c are produced by ***P***. The experimental results shown in Figs 7 and 8 coincide with what is explained above using the model diagrams in Fig. 9.

The shear stress on each slip plane in Fig. 9a contributes to enlargement of the scratched track, whereas in the $[2\,\bar{1}\,\bar{1}]$scratch shown in Fig. 9b the stress ***P*** acts both on the $\{1\,1\,1\}$ planes which diverge and converge to the inside of the material. Therefore, in this case the effect of the shear stress acting to enlarge the track is theoretically less than in the case of the $[\bar{2}\,1\,1]$ scratch. That is, the width of the scratched track and the area deformed plastically in the $[2\,\bar{1}\,\bar{1}]$ scratch are smaller than those in the $[\bar{2}\,1\,1]$ scratch. The reasons for this anisotropy are discussed below in section 3.3 from the viewpoint of interactions between dislocations.

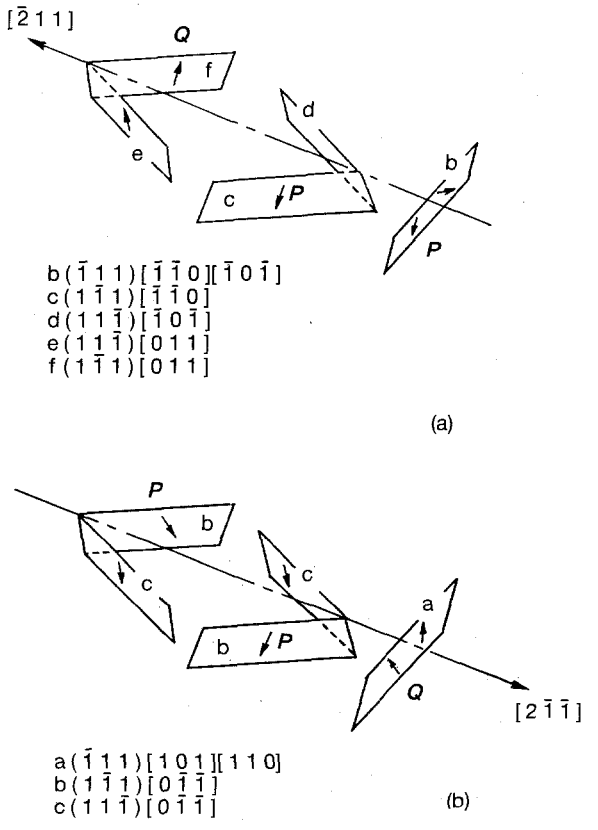

Figure 9 Preferred slip systems in scratch on (1 1 1) face ⟨2 1 1⟩ direction. Scratched direction: (a) $[\bar{2}\,1\,1]$, (b) $[2\,\bar{1}\,\bar{1}]$.

3.2. Dislocation distributions in the ⟨2 1 1⟩ scratch

In order to examine the magnitude of the area where plastic deformation was formed by the scratch, the dislocation density was measured in the same manner as used in static indentation tests [9]: every time a surface layer of 8 μm thickness was removed by electrolytic polishing, the number of etch pits per unit area was counted on the revealed surface.

Fig. 10 shows the relation obtained between dislocation density and distance from the centre of the track under a load of 1.0 N. The result, that the dislocation density decreases monotonously as the distance increases, shows a similar tendency to the case of indentation [9].

The range of the effect of the scratch extends to a distance of 200 μm from the centre of the track. Fig. 11a and b show the isopleth curves of dislocation density inside the material. These are obtained from the results shown in Fig. 10. With reference to the former results obtained in indentation tests [9], it is confirmed that the curves of dislocation density have the same tendencies, and that the depth of the plastically deformed area below the scratched track is also almost the same as in the case of indentation.

These results in Fig. 11 represent the distribution of dislocation density on the $(\bar{2}\,1\,1)$ face which is perpendicular to the scratched surface, and also represent the dimensions of the deformed area inside the crystal. Few differences in the tendency of the distribution curve are observed between Fig. 11a and b. For a scratch in the $[2\,\bar{1}\,\bar{1}]$ direction, it was observed that the width of the track and the area of the deformed region inside the crystal are a bit smaller than those in the $[\bar{2}\,1\,1]$ scratch. This means that the deformed area on the scratched surface corresponds to that on the $\{2\,1\,1\}$ face inside the crystal.

3.3. Deformation pattern inside crystal

In order to observe the dislocation pattern inside the crystal, the test piece scratched on the (1 1 1) face was cut using electrical discharge machining, and one of the slip planes $(1\,\bar{1}\,\bar{1})$ was revealed. This slip plane intersects the (1 1 1) face at an angle of 70.5° as illustrated in Fig. 12.

An example of the results obtained under load of 10.0 N is shown in Fig. 13. The semi-elliptic area (A) just below the scratched track is subjected to large deformation and is of high dislocation density. As a result, etching is allowed to proceed extremely far, and pits cannot be detected.

The dislocation rows distribute symmetrically with the track and intersect the scratched surface at 60° angles. Also, dislocation rows which are parallel to the surface are observed. These facts mean that dislocations are rather active on two different triangular

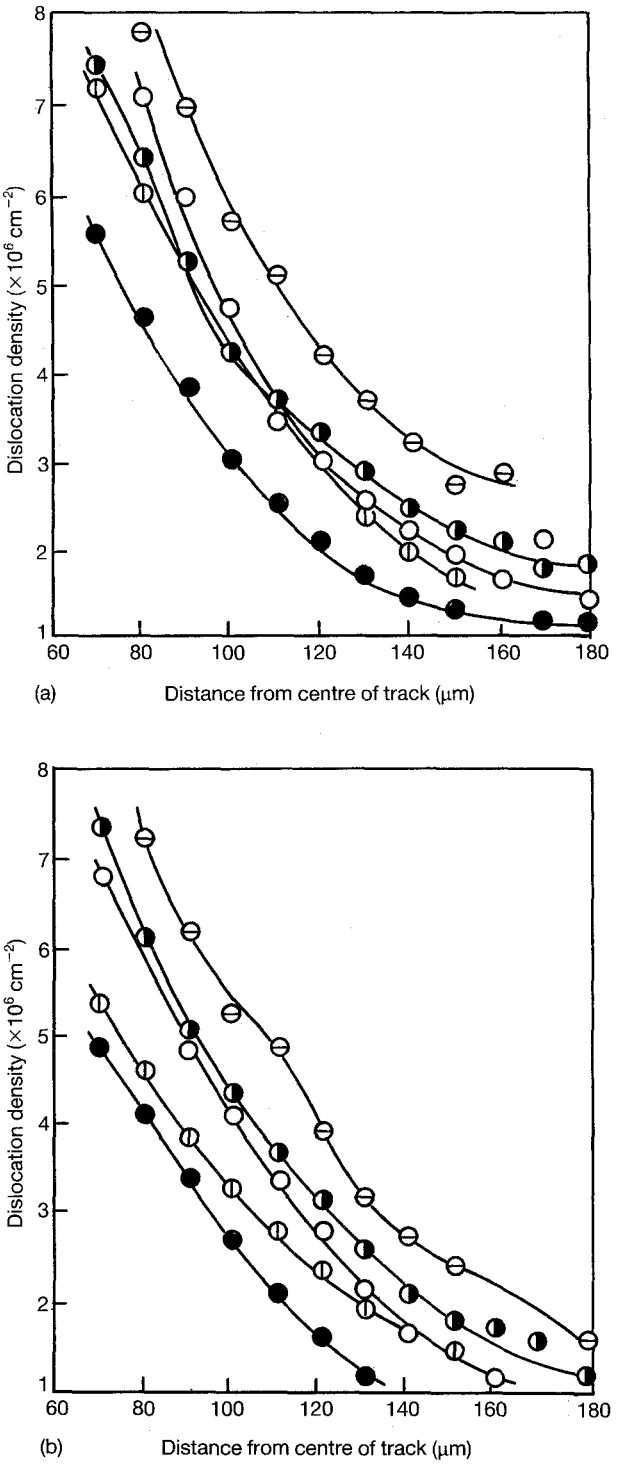

Figure 10 Relation between dislocation density and distance from centre of track under load of 1.0 N scratch: (a) [$\bar{2}$ 1 1], (b) [2 $\bar{1}$ $\bar{1}$]. Depth (μm): (○) 0, (⊕) 8, (⊖) 16, (◑) 28, (●) 40.

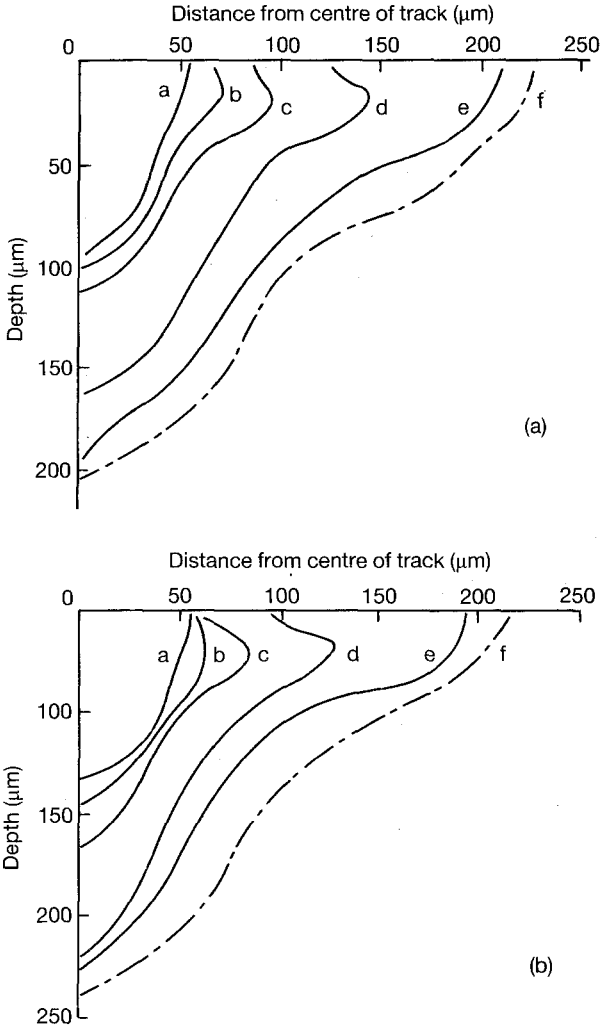

Figure 11 Isopleths of dislocation density under 1.0 N scratches: (a) [$\bar{2}$ 1 1], (b) [2 $\bar{1}$ $\bar{1}$]. Dislocation density (cm^{-2}): curve a 1×10^8, curve b 1×10^7, curve c 6×10^6, curve d 3×10^6, curve e 1×10^6, curve f 5×10^5.

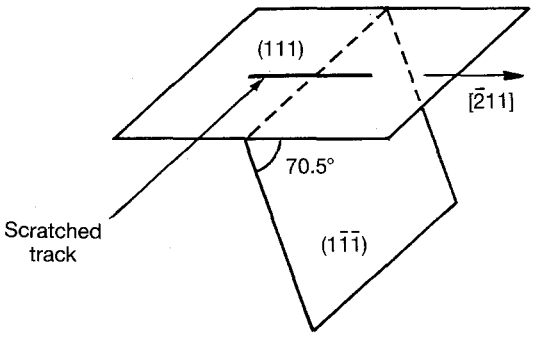

Figure 12 Scratched surface (1 1 1) and cross-section (1 $\bar{1}$ $\bar{1}$).

pyramidal faces. The dislocation rows 1–1′ and 2–2′ in Fig. 13 show individual components of the two different pyramids. Furthermore, the above-mentioned fact confirms that plastic deformations are formed along the scratched direction with a series of deformations produced by indentation with the spherical indentor. As mentioned in section 3.1., it is not only one, but several slip systems that contribute to the formation of the scratched track. Therefore there should be interactions among the dislocation motions. The behaviour of the dislocations in the case of a [2 $\bar{1}$ $\bar{1}$] scratch on the (1 1 1) face of Cu–Al single crystals is discussed in what follows. Two active slip systems (1 $\bar{1}$ 1) [0 $\bar{1}$ $\bar{1}$] and (1 $\bar{1}$ $\bar{1}$) [1 0 1] will be discussed.

Dislocations which are represented by $(a/2)$ [0 $\bar{1}$ $\bar{1}$] and $(a/2)$ [1 0 1] could possibly be resolved as follows:

$$(a/2)\,[0\,\bar{1}\,\bar{1}] \rightarrow (a/6)\,[1\,\bar{1}\,\bar{2}] + (a/6)\,[\bar{1}\,\bar{2}\,\bar{1}]$$

$$(a/2)\,[1\,0\,1] \rightarrow (a/6)\,[1\,\bar{1}\,2] + (a/6)\,[2\,1\,1]$$

where a is the lattice constant. When these partial dislocations intersect each other, the following reactions will occur to form dislocations which are not in existence on the slip planes, which are so-called

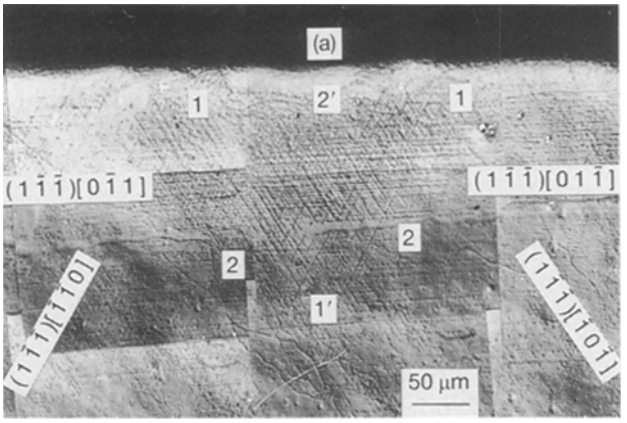

Figure 13 Dislocation structures produced on cross-section (1 1 1).

"sessile dislocations".

$$(a/6)\,[1\,\bar{1}\,\bar{2}] + (a/6)\,[1\,\bar{1}\,2] \rightarrow (a/3)\,[1\,\bar{1}\,0]$$

or

$$(a/6)\,[\bar{1}\,\bar{2}\,\bar{1}] + (a/6)\,[2\,1\,1] \rightarrow (a/6)\,[1\,\bar{1}\,0]$$

Therefore these dislocations formed by intersections are regarded as contributing to strain-hardening due to the scratch.

Similar reactions among the dislocations are expected to take place on the intersection line of the (1 1 $\bar{1}$) and (1 $\bar{1}$ $\bar{1}$) slip planes. On the other hand, when [$\bar{2}$ 1 1] is taken as the scratched direction, the principal slip systems will be (1 $\bar{1}$ 1) [$\bar{1}$ $\bar{1}$ 0] and (1 1 $\bar{1}$) [$\bar{1}$ 0 $\bar{1}$]. Dislocations which belong to these slip systems are decomposed into partial dislocations as follows:

$$(a/2)\,[\bar{1}\,\bar{1}\,0] \rightarrow (a/6)\,[1\,\bar{2}\,\bar{1}] + (a/6)\,[\bar{2}\,\bar{1}\,1]$$

$$(a/2)\,[\bar{1}\,0\,\bar{1}] \rightarrow (a/6)\,[\bar{1}\,1\,\bar{2}] + (a/6)\,[\bar{2}\,1\,\bar{1}]$$

However, even if these decomposed dislocations intersect on the intersection lines of slip planes, the following reactions would never occur, because the dislocation energy on the right-hand side is greater than that on the left:

$$(a/6)\,[1\,\bar{2}\,\bar{1}] + (a/6)\,[\bar{1}\,1\,\bar{2}] \rightarrow (a/2)\,[0\,\bar{1}\,\bar{1}]$$

$$(a/6)\,[\bar{2}\,\bar{1}\,1] + (a/6)\,[\bar{2}\,1\,\bar{1}] \rightarrow (2a/3)\,[\bar{1}\,0\,0]$$

In this case, therefore, sessile dislocations will not be formed as observed in the case of the [2 $\bar{1}$ $\bar{1}$] scratch, and instead of them, intersections among the "extended dislocations" are sure to originate. Even though such intersections are regarded as contributing to strain-hardening when the scratched track is formed, their effects will be less than those of sessile dislocations.

In section 3.1. it was shown that the width of scratched track and the range of plastic deformation in a [$\bar{2}$ 1 1] scratch are larger than those in a [2 $\bar{1}$ $\bar{1}$] scratch. The reason for this was explained from the viewpoint of the relation of stress vectors and slip systems. Hence the above-mentioned difference in mechanism of interaction among the dislocations, i.e. in the degree of strain-hardening, should be added as one of the reasons for the difference in the anisotropy of deformation.

4. Conclusions

From the results of scratch tests with a spherical indentor on the (1 1 1) face of α-Cu–Al single crystals, the following conclusions were obtained.

1. The magnitude of macroscopic deformation observed on the scratched surface does not always correspond to that of microscopic deformation at the dislocation level.
2. The width of scratched track and the range of plastic deformation in a [$\bar{2}$ 1 1] scratch are larger than those in a [2 $\bar{1}$ $\bar{1}$] scratch. The differences can be explained in terms of relations between stress vectors and active slip systems. Furthermore, the difference in mechanism of dislocation reaction is also related to the cause of the anisotropy in deformation.
3. The plastic deformation pattern inside the crystal is formed with a series of deformations produced by indentation.
4. The dislocation density on both the scratched surface and the cross-section changes according to the scratched direction.

References

1. E. RABINOWICZ, "Friction and Wear of Materials" (Wiley, London 1965).
2. M. SODA and J. SATO, *J. Jpn. Soc. Lub. Engrs* **11** (1969) 335.
3. J. M. BAILEY and A. T. GWATHMEY, *ASLE Trans.* **5** (1962) 45.
4. R. P. STEIJN, *Wear* **7** (1964) 48.
5. M. BARQUINS, M. KENNEL and R. COURTEL, *ibid.* **11** (1968) 87.
6. K. F. DUFRANE and W. A. GLAESER, *ibid.* **37** (1976) 21.
7. M. V. SWAIN, *ibid.* **48** (1978) 173.
8. M. F. AMATEAU and J. W. SPRETNAK, *J. Appl. Phys.* **34** (1963) 2340.
9. S. KOBAYASHI, T. HARADA and S. MIURA, *J. Mater. Sci.* **26** (1991) 3945.
10. M. SODA and J. SATO, *Trans. Jpn. Soc. Mech. Engrs.* **40** (1964) 2381.

Received 13 March 1992
and accepted 25 January 1993